

Interacting bosons in two-dimensional flat band systems

Petra Pudleiner,
Institut für Physik, University of Mainz, Germany
Andreas Mielke,
Institut für Theoretische Physik, University of Heidelberg, Germany
18th June 2021

The Hubbard model of bosons on two dimensional lattices with a lowest flat band is discussed. In these systems there is a critical density, where the ground state is known exactly and can be represented as a charge density wave. Above this critical filling, depending on the lattice structure and the interaction strength, the additional particles are either delocalised and condensate in the ground state, or they form pairs. Pairs occur at strong interactions, e.g., on the chequerboard lattice. The general mechanism behind this phenomenon is discussed.

1 Introduction

Flat band systems have been studied extensively in experiment and theory. They are a prototype for strongly correlated systems. Strongly correlated phases of matter emerge in such systems since the interaction, even if it is small, dominates the behaviour. The interaction leads to different phases. Fermions in flat bands are known to show ferromagnetism [1, 2, 3] and ferrimagnetism [4], for a review we refer to [5]. More recently, bosons in flat bands have been studied, esp. the question of Bose condensation [6] and the emergence of topologically ordered phases such as lattice versions of fractional quantum Hall states (see e.g. [7, 8, 9]) are important here. Hard-core bosons can be mapped to spin systems, which as well have been investigated, see e.g. [10, 11].

Promising experiments to realise such systems are ultra-cold atoms in optical lattices; as they provide a perfect implementation of the Hubbard model. Optical lattices might be viewed as quantum simulators and are realised by counter-propagating laser beams forming a periodic microtrap for the atoms. These experiments enable the control of a large number of parameters as the potential depth or the lattice geometry itself, see e.g. [12, 13, 14, 15].

For bosons in a flat band, different phases may occur. A especially interesting question is whether Bose condensation occurs. This question was, to our knowledge, first investigated by Huber et al. [6] for bosons on a kagomé lattice. The kagomé lattice is the line graph of the hexagonal lattice [1] and thus a prototype of a larger class of lattices. For these and similar lattices, the dimensionality is important. This was already shown by Huber et al. [6]. They compared the one-dimensional saw-tooth chain, the line graph of a decorated chain, with the kagomé lattice. Both lattices have an ordered ground state at some critical filling ρ_c : a charge density wave (CDW). Adding further particles to the CDW destroys the

order in the one-dimensional case. Domain walls appear, which can freely move, and the system becomes a Luttinger liquid [6]. This result holds at weak interaction. In the hard-core limit, a two-body bound state is formed which can move through the lattice [16, 17, 18]. On the kagomé lattice, in contrast, domain walls are less favourable than extended states. The CDW ground state on the kagomé lattice is three-fold degenerate. Each of these states has interstitial sites which are unoccupied. The additional particles have a high mobility and probability to move on the interstitial sites. A small but finite density of additional particles form a condensate. The underlying CDW states remain intact for densities above but close to the critical density and break down at higher densities [6]. These results hold for weakly interacting bosons. For strongly interacting bosons, esp. for hard-core bosons, other states may be favourable.

Several questions arise from these results. Since the kagomé lattice is a prototype of a larger class of lattices, one may ask if the results are true on other line graphs of two dimensional bipartite lattices. Another important member of this class is the chequerboard lattice. For the chequerboard lattice, the CDW state at the critical density is two-fold degenerate and there are no interstitial sites [19]. The first question therefore arises, whether on the chequerboard lattice the physics of weakly interacting bosons is the same as on the kagomé lattice. A second question is whether for strongly interacting bosons on one of these lattices bound states occur, as in the one-dimensional system. A third question is, what happens in three dimensions.

In this paper, we concentrate on line graphs of two dimensional bipartite lattices, for several reasons. On this class of lattices, the flat band contains strictly localised states. We will briefly sketch them and their properties in the next section. For details we refer to [19, 20]. Each finite face of the two dimensional bipartite lattices is surrounded by a cycle with an even number of sites. In [20] it was shown that the states which are localised on these cycles are linearly independent and complete. They form a basis, but not an orthonormal basis, which makes it difficult to deal with them. For that reason, we follow the idea of Huber et al. [6] and introduce a Wannier basis. The Wannier states are as well localised, but not strictly on few lattice sites. They fall of algebraically. Similar to the approach by Huber et al. we use the Wannier states in Sect. 3 to derive an effective Hamiltonian for weakly interacting bosons on the chequerboard lattice. It turns out that the essential physics for weak interactions is the same as on the kagomé lattice.

Let us mention that the algebraic decay of the Wannier states was as well used by Chalker et al. [21] in their investigation of disorder and localisation in two-dimensional flat-band systems.

In Sect. 4 we study the case of hard-core bosons. We use different kinds of variational states, partly by using exact diagonalisations of small separable sub-units of the lattice. On the chequerboard lattice, it turns out that pairs of bosons are formed. On the kagomé lattice, the pair states exist as well, but have not the lowest energy. The ground state on small separable sub-units of the lattice shows a larger expectation value of the particle number on the interstitial sites. This indicates that on the kagomé lattice the physical picture developed by Huber et al. remains true for strong interactions. The physics of hard-core bosons on the two lattices, kagomé and chequerboard, is thus different. Finally, in Sect. 5 we give some conclusions and discuss open questions.

2 The model

The Bose-Hubbard model on a lattice is defined by the Hamiltonian

$$H = \sum_{x,y \in V} t_{xy} b_x^\dagger b_y + \frac{U}{2} \sum_{x \in V} b_x^\dagger b_x^\dagger b_x b_x, \quad (1)$$

where V is the set of lattice sites. The interaction $U > 0$ is repulsive. We restrict ourselves to nearest neighbour hoppings, i.e., $t_{xy} = t_{axy}$ where $A = (a_{xy})_{x,y \in V}$ is the adjacency matrix of the lattice, i.e.,

$a_{xy} = 1$ if x, y are nearest neighbours, $a_{xy} = 0$ otherwise. We let $t > 0$ in order to obtain a lowest flat band in the systems we study. We restrict ourselves to lattices which are line graphs of planar, bipartite lattices. Prominent examples are the kagomé lattice, the line graph of the hexagonal lattice, or the chequerboard lattice, the line graph of the square lattice. The usual fermionic Hubbard model has been studied extensively on these lattices and has ferromagnetic ground states [20]. The important feature of line graphs is that the spectrum of the adjacency matrix is bounded from below by -2 and that the eigenvalue -2 has a large degeneracy. Let $|V|$ be the number of lattice sites and n the number of lattice sites per unit cell, then the degeneracy is $|V|/n + 1$. $|V|/n$ is the number of states in the lowest band. The additional state is an element of the next band, which touches the lowest flat band. There is a one-to-one correspondence between the faces of the original planar, bipartite lattice and the localised eigenstates of A . Each face has, since the original lattice is bipartite, an even number of edges. Each edge is, by construction, a vertex of the line graph. A single particle state which has a constant modulus on these edges and an alternating sign is an eigenstate of A with eigenvalue -2 . The eigenstates are linearly independent and thus form a basis of the eigenspace belonging to the eigenvalue -2 . Fig. 1 illustrates the procedure for the chequerboard lattice.

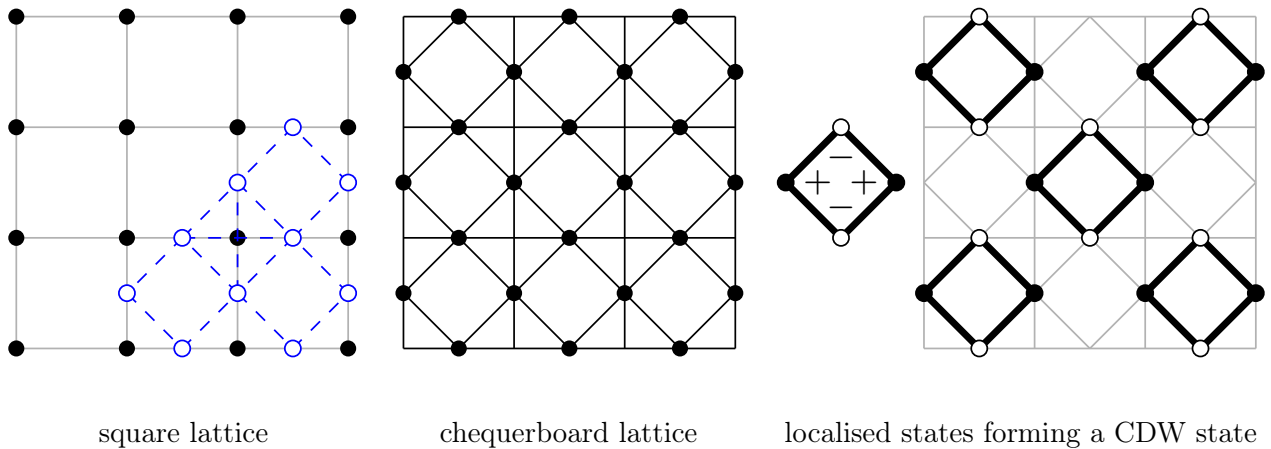


Figure 1: Illustration of the construction of the chequerboard lattice as the line graph of the square lattice and localised states belonging to the faces.

Let us denote the original bipartite planar lattice as G . It consists of two sub-lattices, G_1 and G_2 . Formally, each edge of the original bipartite planar lattice can be oriented to point from G_1 to G_2 . Further, each face can be oriented clockwise. Since the vertices x correspond to edges in G , we define for each face f

$$s_{fx} = \begin{cases} 1, & \text{if } x \text{ belongs to the} \\ & \text{boundary of } f \text{ and points} \\ & \text{into the direction of } f, \\ -1, & \text{if } x \text{ belongs to the} \\ & \text{boundary of } f \text{ and points} \\ & \text{into the opposite direction} \\ & \text{of } f, \\ 0, & \text{otherwise,} \end{cases} \quad (2)$$

and the creation operators

$$b_f^\dagger = \frac{1}{\sqrt{|f|}} \sum_{x \in V} s_{fx} b_x^\dagger. \quad (3)$$

Due to the local structure of b_f^\dagger , it is possible to construct multi-particle ground states for the Bose-Hubbard Hamiltonian for densities below some critical density ρ_c . For low densities, there exist many such states. Each set F of non-touching faces yields a ground state $|F\rangle = \prod_{f \in F} b_f^\dagger |0\rangle$. In fact, one can show that these states only form a subset of all ground states at low densities. A complete rigorous description of all multi-particle ground states below a certain critical density ρ_c has been given in [19] for all line graphs of planar bipartite lattices. The critical density is given by a close packing of non-touching faces. Depending on the lattice, there may be more than one close packing. The checkerboard lattice has two such close packings. This procedure yields thus one or more charge density wave (CDW) states. On the checkerboard lattice, the critical density is $\rho_c = \frac{1}{4}$. There are two such states, one of them is depicted in Fig. 1. We denote the corresponding two subsets by F_1^c and F_2^c .

Above the critical density it has to be examined whether the CDW is destroyed completely or is disturbed merely locally. Therefore, the energies of these configurations have to be compared for a lattice filling with one further particle. In the case of the kagomé lattice and for weak interactions, Huber et al. [6] showed that the additional particles become delocalised and form a condensate. The kagomé lattice has a critical density of $\rho_c = \frac{1}{9}$ and three degenerate CDW ground states at the critical filling. As a consequence, a CDW state on the kagomé lattice has interstitial sites, which belong to no occupied face. In this aspect, it differs to the checkerboard lattice, on which a CDW state has no interstitial sites.

3 Weakly interacting model

In this section, we study the Bose Hubbard model on the checkerboard lattice for weak interaction using a variational approach similar to the one used by Huber et al. [6] for the kagomé lattice. This section contains no essentially new results, we just confirm that the results in [6] can be extended to the checkerboard lattice and presumably to any other lattice which is a line graph of a planar bipartite lattice.

The main problem with the basis states b_f^\dagger constructed above is that these states are not orthogonal. To keep the property of localised states and to deal with an orthonormal basis, we follow Huber et al. and construct a basis of Wannier states. This allows us to project to the lowest band and to derive an effective Hamiltonian, which can be treated further. As a starting point, we write the hopping part of the Hamiltonian (1) as

$$H_{\text{hop}} = t \sum_{\mathbf{k}} \begin{pmatrix} b_{A,\mathbf{k}}^\dagger & b_{B,\mathbf{k}}^\dagger \end{pmatrix} \cdot \begin{pmatrix} z_1(k_1) - 2 & z_2^*(k_1, k_2) \\ z_2(k_1, k_2) & z_1(k_2) - 2 \end{pmatrix} \begin{pmatrix} b_{A,\mathbf{k}} \\ b_{B,\mathbf{k}} \end{pmatrix}, \quad (4)$$

with

$$z_1(k_\nu) = e^{ik_\nu} + e^{-ik_\nu} + 2 \quad (5)$$

$$z_2(k_1, k_2) = 1 + e^{ik_1} + e^{-ik_2} + e^{i(k_1 - k_2)}, \quad (6)$$

using $k_\nu = \mathbf{k} \cdot \mathbf{a}_\nu$ for $\nu \in \{1, 2\}$. The vector \mathbf{k} belongs to the first Brillouin zone. The two vectors \mathbf{a}_ν are shown in Fig. 2. The eigenvalues are $-2t$ and $2t[1 + \cos(k_1) + \cos(k_2)]$ and are plotted in Fig. 2 as well.

We now construct the Wannier basis for the lower flat band. The Wannier operators are

$$W_i^\dagger = \sum_j \left[w_A^*(\mathbf{r}_j - \mathbf{r}_i) b_{A,j}^\dagger + w_B^*(\mathbf{r}_j - \mathbf{r}_i) b_{B,j}^\dagger \right] \quad (7)$$

$$w_A(\mathbf{r}_i) = \int \frac{d^2k}{(2\pi)^2} e^{i\mathbf{k}\mathbf{r}_i} \frac{1 + e^{-ik_2}}{[4 + 2\cos(k_1) + 2\cos(k_2)]^{\frac{1}{2}}} \quad (8)$$

$$w_B(\mathbf{r}_i) = - \int \frac{d^2k}{(2\pi)^2} e^{i\mathbf{k}\mathbf{r}_i} \frac{1 + e^{-ik_1}}{[4 + 2\cos(k_1) + 2\cos(k_2)]^{\frac{1}{2}}}, \quad (9)$$

with the lattice vector $\mathbf{r}_i = \sum_j m_{j\nu} \mathbf{a}_\nu$ and integers $m_{i\nu}$. The index i runs over all elementary cells of the lattice. The creation operators $b_{A/B,i}^\dagger$ create bosons on the lattice site A or respectively B in the elementary cell i . This state W_i^\dagger involves bosons of all lattice sites, weighted with the appropriate coefficients which depend on the distance to the elementary cell i . These coefficients decay with increasing distance at least by $1/|\mathbf{r}|$.

Using the Wannier states, we write the local operators as

$$b_{A(B),i}^\dagger = \sum_j [w_{A(B)}(\mathbf{r}_i - \mathbf{r}_j) W_j^\dagger + \text{higher band}]. \quad (10)$$

Projecting onto the flat band means neglecting the contribution of the higher band. This corresponds to the low-energy regime for a weakly interacting system. We insert Eq. (10) into the Hamiltonian (1) and remove the energy offset $-2tN$. The largest term in the resulting Hamiltonian is an on-site repulsion. It is much larger than all the other terms. Following Huber et al. [6], we replace it by a hard core interaction. The remaining terms are interactions and assisted hoppings. Due to the decay of the Wannier functions, the coefficients decay with increasing distance. The first leading terms are

$$H_{\text{eff}}^{(w)} = P_0 U \sum_{i,\nu \in (1,2)} W_i^\dagger W_i \left\{ A_{1,i} + [A_{2,i} + \text{h.c.}] \right\} P_0, \quad (11)$$

where

$$A_{1,i} = \frac{I_1}{2} W_{i\pm\mathbf{a}_\nu}^\dagger W_{i\pm\mathbf{a}_\nu} + 2I_2 W_{i\pm\mathbf{a}_\nu}^\dagger W_{i\mp\mathbf{a}_\nu} + 2I_3 W_{i\pm\mathbf{a}_\nu}^\dagger [W_{i\pm\mathbf{a}_{\nu+1}} + W_{i\mp\mathbf{a}_{\nu+1}}] \quad (12)$$

$$\begin{aligned}
A_{2,i} &= I_2 W_{i\pm\mathbf{a}_\nu}^\dagger W_{i\pm 2\mathbf{a}_\nu} \\
&+ I_3 W_{i\pm\mathbf{a}_\nu}^\dagger \left[W_{i\pm\mathbf{a}_\nu\pm\mathbf{a}_{\nu+1}} + W_{i\pm\mathbf{a}_\nu\mp\mathbf{a}_{\nu+1}} \right] \\
&+ I_4 W_{i\pm\mathbf{a}_\nu}^\dagger \left[W_{i\mp\mathbf{a}_\nu\mp\mathbf{a}_{\nu+1}} + W_{i\mp\mathbf{a}_\nu\pm\mathbf{a}_{\nu+1}} \right. \\
&\quad \left. + W_{i\pm 2\mathbf{a}_\nu\pm\mathbf{a}_{\nu+1}} + W_{i\pm 2\mathbf{a}_\nu\mp\mathbf{a}_{\nu+1}} \right] \\
&+ I_5 W_{i\pm\mathbf{a}_\nu}^\dagger \left[W_{i\pm 3\mathbf{a}_\nu} + W_{i\mp 2\mathbf{a}_\nu} \right]
\end{aligned} \tag{13}$$

The coefficients are

$$\begin{aligned}
I_1 &= 2w_A(0)^4 && \approx 0.105 \\
I_2 &= 2w_A(0)^3 w_A(-\mathbf{a}_2) && \approx -0.018 \\
I_3 &= 2w_A(0)^3 w_A(\mathbf{a}_1) && \approx -0.013 \\
I_4 &= 2w_A(0)^3 w_A(\mathbf{a}_1 - \mathbf{a}_2) && \approx 0.008 \\
I_5 &= 2w_A(0)^3 w_A(-2\mathbf{a}_2) && \approx 0.006.
\end{aligned} \tag{14}$$

P_0 projects onto states with not more than one boson in a state W_i^\dagger .

Again following Huber et al. [6], we use a variational ansatz for the ground state above ρ_c of the form

$$\begin{aligned}
|\vartheta_1 \vartheta_2 \varphi_1 \varphi_2\rangle &= \prod_{\alpha=1}^2 \prod_{i \in F_\alpha} \left[\cos(\vartheta_\alpha/2) \right. \\
&\quad \left. + e^{i\varphi_\alpha} \sin(\vartheta_\alpha/2) W_i^\dagger \right] |0\rangle.
\end{aligned} \tag{15}$$

The ansatz contains two CDW states $|\pi 0 0 0\rangle = W_1^\dagger |0\rangle$ and $|0 \pi 0 0\rangle = W_2^\dagger |0\rangle$ with $W_\alpha^\dagger = \prod_{i \in F_\alpha} W_i^\dagger$, both with filling ρ_c . Taking the expectation value of the Hamiltonian (11) yields

$$\begin{aligned}
\langle \Psi | H_{\text{eff}}^{(w)} - \mu \hat{N} | \Psi \rangle &= U \left[2A_1 \sin^2 \frac{\vartheta_1}{2} \sin^2 \frac{\vartheta_2}{2} \right. \\
&+ B_1 \left[\sin^2 \vartheta_1 \sin^2 \frac{\vartheta_2}{2} + \sin^2 \vartheta_2 \sin^2 \frac{\vartheta_1}{2} \right] \\
&+ B_2 \left[\sin^2 \vartheta_1 \sin^2 \frac{\vartheta_1}{2} + \sin^2 \vartheta_2 \sin^2 \frac{\vartheta_2}{2} \right] \\
&+ B_3 \cos(\varphi_1 - \varphi_2) \sin \vartheta_1 \sin \vartheta_2 \left[\sin^2 \frac{\vartheta_1}{2} \right. \\
&\quad \left. + \sin^2 \frac{\vartheta_2}{2} \right] \left. \right] - \frac{\mu}{2} \left[\sin^2 \frac{\vartheta_1}{2} + \sin^2 \frac{\vartheta_2}{2} \right].
\end{aligned} \tag{16}$$

The coefficients are combinations of the interaction coefficients I_i . They have the following values

$$\begin{aligned}
A_1 &\approx 0.0527 & B_2 &\approx -0.0002 \\
B_1 &\approx -0.0138 & B_3 &\approx -0.0072.
\end{aligned} \tag{17}$$

Eq. (16) is minimised numerically by varying the parameters $\vartheta_{1,2}$, $\varphi_1 - \varphi_2$ and μ ; the latter in order to keep the particle number fixed. The density ρ is varied between the critical filling factor $\rho_c = \frac{1}{4}$ and $\rho = \frac{1}{2}$.

Starting point is the CDW state $W_1^\dagger|0\rangle$ at ρ_c . This enables to determine quantitatively the expectation value of $H_{\text{eff}}^{(w)}$ and by analogy to [6] the order parameter of the CDW

$$\begin{aligned}\psi_{\text{CDW}} &= \frac{\langle \Psi | W_1^\dagger W_1 - W_2^\dagger W_2 | \Psi \rangle}{\langle \Psi | W_1^\dagger W_1 + W_2^\dagger W_2 | \Psi \rangle} \\ &= \frac{\cos \vartheta_1 - \cos \vartheta_2}{\cos \vartheta_1 + \cos \vartheta_2 - 2},\end{aligned}\tag{18}$$

and of the superfluid

$$\psi_{\text{sf}} = \frac{2}{N} \left| \langle \Psi | W_2^\dagger | \Psi \rangle \right| = \frac{1}{2} \left| \sin \vartheta_2 \right|.\tag{19}$$

The results are plotted as a function of the density in Fig. 3. The order parameter of the CDW decreases continuously from 1.0 by increasing the density above the critical filling factor, and conversely the superfluid order parameter grows from 0.001 on. For densities higher than $\rho \approx 0.36$ the order parameter of the CDW abruptly vanishes and the superfluid phase starts to decay.

As the set of variational states is restricted to hard-core bosons we exclude double occupancy. Hence, for large densities this approach is not a sufficient choice for calculations of ground states and will not provide reliable results. Furthermore, the truncation of the Wannier state – regarding only leading terms – also requires adequate low lattice fillings. Huber et al. [6] observed a similar behaviour which might also confirm that we reach a limit of our model at this density regime and do not observe any physical response.

We tested the stability of the approximation in Eq. (11) by taking all coefficients into account up to $0.001U$. We observe a similar result. The onset of the decline for the superfluid order parameter remains more or less unchanged with 0.37. However, the density for which the order parameter of the CDW will be zero is shifted to 0.47. In general, this indicates, nevertheless, the stability of the truncation procedure.

To conclude, the results for the chequerboard lattice are similar to the results for the kagomé lattice derived by Huber et al. [6], although, as pointed out above, there are no interstitial sites on the chequerboard lattice. The essential point is, indeed, that the additional particles are delocalised. These particles have a high mobility and this is energetically favourable to localised states, as pointed out by Huber et al.

4 Strongly interacting model

If U is much larger than t , states where a site is occupied with more than one boson are energetically unfavourable. We take the limit $U \rightarrow \infty$, i.e. hard-core bosons. For densities $\rho < 1$ this means that we project onto the subspace of multi-particle states where each site is occupied with at most one boson. Let $P_{\leq 1}$ be the projector onto this subspace. Then, the Hamiltonian reads

$$H = t P_{\leq 1} \sum_{x,y \in V} a_{xy} b_x^\dagger b_y P_{\leq 1}.\tag{20}$$

4.1 The chequerboard lattice

The CDW is the exact ground state at the critical density [19]. Therefore, as in the case of small U , we use the CDW at the critical density and add one further boson. A first variational ansatz for the ground

state is thus

$$\begin{aligned}
|\phi\rangle &= P_{\leq 1} \sum_{x \in V} \phi_x b_x^\dagger |F_1^c\rangle \\
&= \sum_{f \in F_1^c} \frac{1}{\sqrt{|f|}} \sum_{x, x' \in f, x \neq x'} \phi_x s_{fx'} b_x^\dagger b_{x'}^\dagger \\
&\quad \cdot \prod_{f' \in F_1^c \setminus \{f\}} b_{f'}^\dagger |0\rangle.
\end{aligned} \tag{21}$$

The variation was done on a 20x20 cutout of the chequerboard lattice. For reasons of numerical stability, we choose a symmetric sub-unit of 16 lattice sites containing five faces on which ϕ_x are varied freely and we let $\phi_x = \phi_R$ outside that region. The resulting minimal energy is $-(2|F_1^c| + 0.67)t$ and belongs to a state where the additional particle is localised on one of the faces of the sub-unit which are already occupied. It seems energetically favourable to disturb only one particle instead of four when putting the additional particle on a not occupied face. It seems also energetically favourable to have the additional particle localised and not distributed over many faces.

Since the additional particle is localised on an already occupied face, a second variational ansatz for the ground state is

$$|u, f\rangle = \sum_{e, e' \in f \in F_1^c} u_{ee'} b_e^\dagger b_{e'}^\dagger b_f |F_1^c\rangle, \tag{22}$$

for an arbitrary face of F_1^c . Since all faces are independent, this variational problem is equivalent to solving the problem for two hard-core bosons on a square. The resulting energy is $-2\sqrt{2}t$ for the two hard-core bosons and therefore $-(2|F_1^c| - 2 + 2\sqrt{2})t = -(2|F_1^c| + 0.83)t$. If this was the exact ground state, it would be degenerate with a degeneracy $|F_1^c|$. As a consequence of this variational ansatz, we obtain an exact upper limit for the ground state energy per particle $e_0(\rho)$ for hard-core bosons on the chequerboard lattice at density ρ to be

$$e_0(\rho) \leq -[2\rho_c + (2\sqrt{2} - 2)(\rho - \rho_c)]t, \tag{23}$$

which holds for $\rho_c \leq \rho < 2\rho_c$. The number of states at or below that energy must be equal or above the number of occupied faces.

As a further test of the ansatz, we look at the next non-trivial sub-unit, depicted in Fig. 4. The exact ground state with four particles is the state where the four faces in the corners are occupied, depicted as circles in Fig. 4. We now put a fifth boson into the sub-unit. Following the argument above, we conclude that there are at least four ground states with an energy below $-(6 + 2\sqrt{2})t = -8.83t$. A numerical diagonalisation of the system yields, indeed, exactly four states with energies below that value. These energies are $-9.016t$, $-9.022t$ (two-fold degenerate), and $-9.081t$. The corresponding eigenstates have a large overlap with combinations of the four variational states. They thus show a similar behaviour as it was observed in different one-dimensional models [16, 17, 18]. Pairs of bosons are formed.

Since this sub-unit shares no sites with other occupied faces, we can use this result as a new upper variational limit for densities between ρ_c and $\frac{5}{4}\rho_c$,

$$e_0(\rho) \leq -[2\rho_c + 1.081(\rho - \rho_c)]t. \tag{24}$$

4.2 The kagomé lattice

Whereas at weak interactions, physics of hard-core bosons on the chequerboard and the kagomé lattice are similar, there may be a difference at strong interactions. On the kagomé lattice a CDW ground state

at the critical density has interstitial sites, whereas on the chequerboard lattice there are no interstitial sites.

On the kagomé lattice, the smallest building block is a hexagon. One particle on the hexagon has an energy of $-2t$. If we put two hard-core bosons on a hexagon, the energy is $-2\sqrt{3}t$.

The smallest non-trivial sub-unit of the kagomé lattice consists of one hexagon, surrounded by six triangles and three non-touching hexagons, as depicted in Fig. 5.

Three hard-core bosons on this sub-unit are placed on the three outer hexagons; the corresponding state is the only ground state on this sub-unit with energy $-6t$. This state has three interstitial sites. The ground state with four particles on this sub-unit must have an energy below $-(4 + 2\sqrt{3})t = -7.46t$ and following our variational argument, there are at least three eigenstates below this energy.

A numerical diagonalisation of the sub-unit with four particles shows that there are three almost degenerate states with energies between $-7.55t$ and $-7.56t$ and one state, the ground state, with an energy of $-7.66t$. The ground state has a large expectation value of the particle number on the three interstitial sites of the inner hexagon, whereas this expectation value is small on the other three low eigenstates. The overlap of the ground state, with one of the states where two particles are on a hexagon, is only 0.085. The other three exact eigenstates with energies below $-(4 + 2\sqrt{3})t$ have a high overlap with linear combinations of the three states with two particles on a hexagon. The overlap lies above 0.95. This shows, that linear combinations of the variational states, where the additional hard-core boson is put on one of the occupied hexagons, describe these three low energy states well. However, in the true ground state of the sub-unit the additional particle moves on the interstitial sites and is not localised on one of the occupied hexagons.

This argument shows that interstitial sites on the kagomé lattice are important if hard-core bosons are added to one of the ground states at the critical filling. This suggests that the argument by Huber et al. [6] may remain correct in the regime of strong interaction. The additional bosons move mainly on the interstitial sites and form a condensate at densities slightly above the critical density.

4.3 Other line graphs

The same arguments apply to line graphs of other bipartite plane lattices. If the faces of the underlying bipartite plane lattice form a two-colour map, the CDW states are at most two-fold degenerate. Since each edge belongs to two faces, there are no interstitial sites. On the other hand, if three or more colours are needed to colour the faces of the underlying bipartite plane lattice, the CDW states have interstitial sites. This is true for infinite lattices and also for finite sub-units. In the latter case the outer faces has to be coloured as well. Therefore, the sub-units should be chosen such that they need the same number of colours as the original lattice.

An example for the case with more than two colours is the so called truncated square tiling or 4.8^2 -tiling, a bipartite plane lattice formed of octagons and squares. Hard-core bosons on its line graph have a unique CDW ground state with one boson on each square. There are interstitial sites stemming from the additional edges of the octagons. The smallest non-trivial sub-unit consists of one octagon surrounded by four non-touching squares. Putting five hard-core bosons on this sub-unit, we expect at least four ground states with an energy less than $-(6 + 2\sqrt{2})t$, corresponding to the four states where the additional particle is put on one of the already occupied squares. A numerical diagonalisation of the sub-unit yields eight eigenstates with an energies less than $-(6 + 2\sqrt{2})t$. As for the kagomé lattice, the ground state has a large expectation value of the particle number on the four interstitial sites. Let us mention that in this case it might even be favourable to put two bosons on the interstitial site, because two hard-core bosons on the octagon have an energy of $-\sqrt{10 + 2\sqrt{5}}t = -3.804t$. This state contributes to the low lying eigenstates as well. The analysis on this sub-unit thus shows that the ground state is dominated by interstitial sites.

An example where the faces of the underlying bipartite plane lattice form a two-colour map, like for the

square lattice, can be constructed from the triangular lattice. We put an additional lattice site on each edge of the triangular lattice. The resulting lattice is a bipartite plane lattice. Its line graph has hexagons connected via complete graphs with six vertices, similar to the kagomé lattice, where the hexagons are connected via complete graphs with three vertices. Two particles on a hexagon have the energy $-2\sqrt{3}$. Let us take a sub-unit with four hexagons, one in the middle surrounded by three non-touching hexagons. Since there are three non-touching hexagons, we expect at least three eigenstates with energies below $-(4 + 2\sqrt{3})t$. The exact diagonalisation yields four such eigenstates. The three lowest states have, again, a large overlap between 0.66 and 0.88 with linear combinations of the states where the additional particle is put on a hexagon. The fourth eigenstate appears because of the large boundary of the sub-unit. Indeed, if we put two particles on the inner hexagon and two particles on the ring of 12 sites forming the boundary, we get a variational state with an energy of $-7.36t$, only slightly above $-(4 + 2\sqrt{3})t$. This additional variational state has thus two bound pairs of bosons, in contrast to the three others with one bound pair, and a large overlap with two of the four low lying eigenstates. Thus, in the ground state and in the three low lying eigenstates of this sub-unit, bound pairs of bosons are formed as for the checkerboard lattice.

There exist one-dimensional systems where these arguments apply as well. Consider for instance the line graph of the square chain, a lattice of two chains of corner sharing triangles. The square chain needs indeed three colours because the two outer faces cannot be coloured with the same colour as the squares. Thus, the CDW states have interstitial sites. A numerical diagonalisation shows indeed that for hard-core bosons, additional particles move on these sites. Let us mention that this one-dimensional lattice is sometimes called kagomé-chain, see e.g. [10]

5 Conclusion and outlook

We showed that weakly interacting bosons on the checkerboard lattice behave similarly to weakly interacting bosons on the kagomé lattice. We essentially confirmed the results obtained by Huber et al. for the kagomé lattice. Above the critical density the additional particles are delocalised and form a condensate.

For hard-core bosons, the situation is different: our results indicate that on the checkerboard lattice the additional particles form pairs of two bound bosons. This is similar to the findings of Phillips et al. for the saw-tooth chain [18]. In contrast to that, on the kagomé lattice the additional particles move on interstitial sites as for weak interaction.

The kagomé lattice and the checkerboard lattice are just examples of two larger classes of two-dimensional lattices with flat bands. The kagomé lattice is a prototype of line graphs of bipartite plane lattices where the faces cannot be coloured with two colours. Instead, three or four colours are needed. For all lattices in this class, the CDW states have interstitial sites and we expect that additional particles will move on these sites, even for strong interactions. The checkerboard lattice is a prototype of line graphs of bipartite plane lattices where the faces form a two-colour map. In that case, since each edge of the original bipartite plane lattice belongs to exactly two faces, the CDW states have no interstitial sites and pairs of bound particles are formed for strong interactions.

There are several questions which remain open. For instance, one may easily construct line graphs of three dimensional lattices like the line graph of the diamond lattice, an analog to the kagomé lattice in three dimensions, or the line graph of the simple cubic lattice. Partly, such lattices can be found in nature. The line graph of the diamond lattice is the octahedral sublattice of a spinel. Being line graphs of bipartite graphs, these lattices have a lowest flat band and localised single particle eigenstates in that band. As in two dimensions, it is possible to construct strictly localised states. As in two dimensions, they are localised on the elementary cycles, squares or hexagons in the two examples. But unfortunately, a complete description of all multi-particle ground states at or below the critical density is not known.

The arguments in [19] do not apply here. Therefore, a discussion of these lattices above the critical filling is out of reach today.

Let us mention that hard-core bosons on graphs is a topic that has recently been discussed in (algebraic) graph theory in connection with the isomorphism problem [22, 23, 24, 25]. Spectral properties of hard-core bosons on a graph can reveal certain properties of the graph which are otherwise difficult to obtain. There is no direct relation between the current paper and these investigations, which mainly deal with strongly regular graphs. Nevertheless, it is interesting to see that here as well a certain spectral property of hard-core bosons is connected to a graph theoretical problem, here the colouring of the faces.

Acknowledgement

A.M. wishes to thank Ehud Altman for stimulating discussions.

Author contribution statement: Both authors contributed equally to the paper.

References

- [1] A. Mielke. *J. Phys. A: Math. Gen.* **24**, 3311–3321 (1991).
- [2] H. Tasaki. *Phys. Rev. Lett.* **69**, 1608 (1992).
- [3] A. Mielke and H. Tasaki. *Commun. Math. Phys.* **158**, 341 (1993).
- [4] E.H. Lieb. *Phys. Rev. Lett.* **62**, 1201 (1989).
- [5] H. Tasaki. *Prog. Theo. Phys.* **99**, 489 (1998).
- [6] S. D. Huber and E. Altman. *Phys. Rev. B* **82**, 184502 (2010).
- [7] Y.F. Wang, Z.C. Gu, C.D. Gong, and D.N. Sheng. *Phys. Rev. Lett.* **107**, 146803 (2011).
- [8] Y.F. Wang, H. Yao, Z.C. Gu, C.D. Gong, and D.N. Sheng. *Phys. Rev. Lett.* **108**, 126805 (2012).
- [9] Z. Liu, E.J. Bergholtz, H. Fan, and A.M. Laeuchli. *Phys. Rev. Lett.* **109**, 186805 (2012).
- [10] J. Schulenburg, A. Honecker, J. Schnack, J. Richter, and H.-J. Schmidt. *Phys. Rev. Lett.* **88**, 167207 (2002).
- [11] M. E. Zhitomirsky and H. Tsunetsugu. *Phys. Rev. B* **70**, 100403(R) (2004).
- [12] M. Greiner, O. Mandel, T. Esslinger, T.W. Hänsch, and I. Bloch. *nature* **415**, 39 (2002).
- [13] I. Bloch. *Nature Physics* **1**, 23 (2005).
- [14] M. Lewenstein, A. Sanpera, V. Ahufinger, B. Damski, A. Sen, and U. Sen. *Adv. Phys.* **56**, 243 (2007).
- [15] I. Bloch, J. Dalibard, and W. Zwerger. *Rev. Mod. Phys.* **80**, 885 (2008).
- [16] S. Takayoshi, H. Katsura, N. Watanabe, and H. Aoki. *Phys. Rev. A* **88**, 063613 (2013)
- [17] M. Tovmasyan, E. P. L. van Nieuwenburg, and S. D. Huber. *Phys. Rev. B* **88**, 220510(R) (2013)
- [18] L.G. Phillips, G. De Chiara, P. Öhberg, and M. Valiente. *Phys. Rev. B* **91**, 054103 (2015).

- [19] J. Motruk and A. Mielke. *J. Phys. A* **45**, 225206 (2012).
- [20] A. Mielke. *J. Phys. A: Math. Gen.* **25**, 4335 (1992).
- [21] J. T. Chalker, T. S. Pickles, and P. Shukla. *Phys. Rev. B* **82**, 104209 (2010)
- [22] K. Audenaert, C. Godsil, G. Royle, and T. Rudolph. *arXiv preprint math/0507251* (2005).
- [23] J. K. Gamble, M. Friesen, D. Zhou, R. Joynt, and S.N. Coppersmith. *Phys. Rev. A* **81**, 052313 (2010).
- [24] S.D. Berry and J.B. Wang. *Phys. Rev. A* **83**, 042317 (2011).
- [25] K. Rudinger, J.K. Gamble, M. Wellons, E. Bach, M. Friesen, R. Joynt, and S.N. Coppersmith. *Phys. Rev. A* **86**, 022334 (2012).

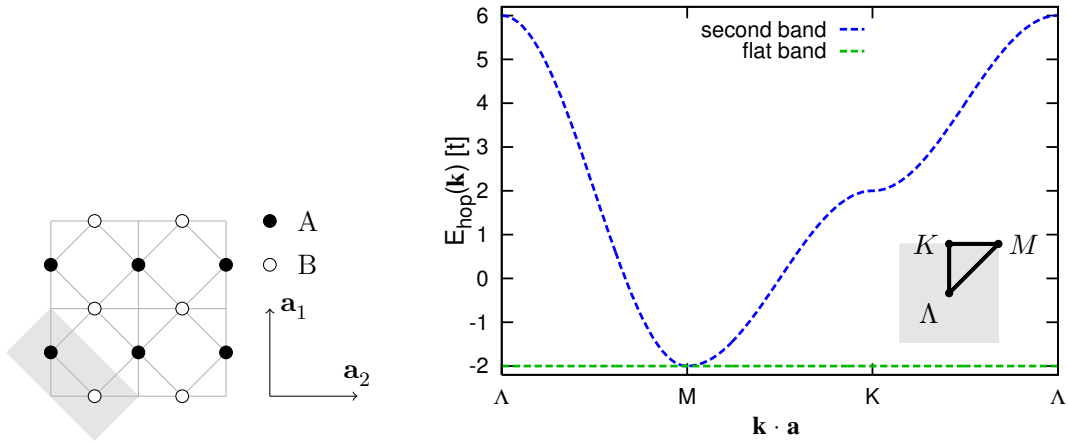


Figure 2: The band structure of the checkerboard lattice in the first Brillouin zone (right) and the choice of the unit cell (left) with the two lattice vectors $\mathbf{a}_{1,2}$ and the two lattice types A and B.

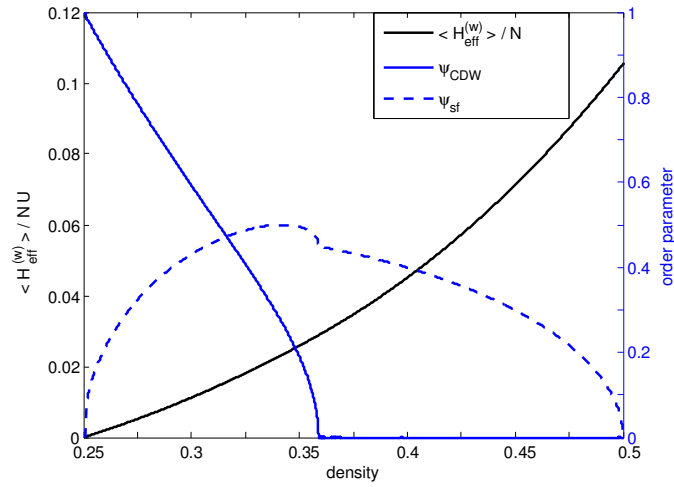


Figure 3: The expectation value of $H_{\text{eff}}^{(w)}$ [cf. Eq. (16)] is plotted on the left y-axis for the parameters obtained by solving the variational problem. Eq. (18) and (19) are likewise depicted on the right y-axis for the order parameter of the CDW and the superfluid, respectively.

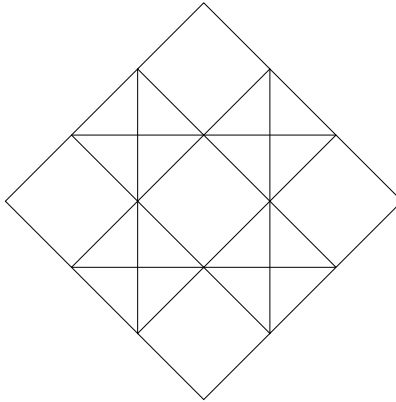


Figure 4: Sub-unit of the chequerboard lattice. The cycles denote the occupied faces. In the exact ground state with four particles, each face is occupied by one boson. In the variational states (22) with five bosons one of the faces is occupied by two bosons.

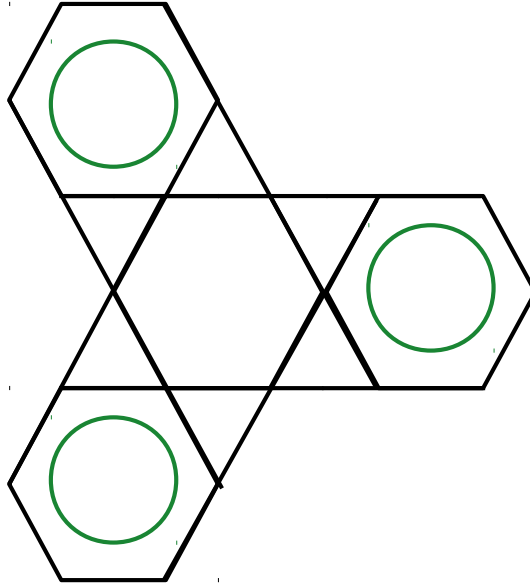


Figure 5: Sub-unit of the kagomé lattice. The cycles denote the occupied faces. In the exact ground state with three particles, each face is occupied by one boson. In the variational states (22) with four bosons one of the faces is occupied by two bosons.